Kinetics and Mechanisms of Catalytic Oxygen Atom Transfer with Oxorhenium(V) Oxazoline Complexes

Joachin Arias, Craig R. Newlands, and Mahdi M. Abu-Omar*,†

Department of Chemistry and Biochemistry, University of California, Los Angeles, 405 Hilgard Avenue, Los Angeles, California 90095-1569

Received August 11, 2000

The rhenium(V) monooxo complexes $(hoz)_2Re(O)Cl$ (**1**) and $[(hoz)_2Re(O)(OH_2)][OTf]$ (**2**) have been synthesized and fully characterized (hoz = 2-(2′-hydroxyphenyl)-2-oxazoline). A single-crystal X-ray structure of **2** has been solved: space group = $P\bar{1}$, $a = 13.61(2)$ Å, $b = 14.76(2)$ Å, $c = 11.871(14)$ Å, $\alpha = 93.69(4)°$, $\beta = 99.43(4)°$, $\gamma = 108.44(4)°$, $Z = 4$; the structure was refined to final residuals $R = 0.0455$ and $R_w = 0.1055$. **1** and **2** catalyze oxygen atom transfer from aryl sulfoxides to alkyl sulfides and oxygen-scrambling between sulfoxides to yield sulfone and sulfide. Superior catalytic activity has been observed for **2** due to the availability of a coordination site on the rhenium. The active form of the catalyst is a dioxo rhenium(VII) intermediate, $[Re(O)_2(hoz)_2]^+$ (**3**). In the presence of sulfide, **3** is rapidly reduced to $[Re(O)(hoz)_2]^+$ with sulfoxide as the sole organic product. The transition state is very sensitive to electronic influences. A Hammett correlation plot with para-substituted thioanisole derivatives gave a reaction constant ρ of -4.6 ± 0.4, in agreement with an electrophilic oxygen transfer from rhenium. The catalytic reaction features inhibition by sulfides at high concentrations. The equilibrium constants for sulfide binding to complex **2** (cause of inhibition), K_2 (L mol^{-1}), were determined for a few sulfides: Me_2S (22 ± 3), Et_2S (14 ± 2), and $^tBu_2S$ (8 ± 2). Thermodynamic data, obtained from equilibrium measurements in solution, show that the S═O bond in alkyl sulfoxides is stronger than in aryl sulfoxides. The Re═O bond strength in **3** was estimated to be about 20 kcal mol^{-1}. The high activity and oxygen electrophilicity of complex **3** are discussed and related to analogous molybdenum systems.

Introduction

One of the fundamental reactions in both chemistry and biology is the transfer of an oxygen atom from a substrate to a transition metal or vice versa (eq 1).[1−4] Many valuable synthetic methodologies in organic oxidation utilize transition-metal catalysts, olefin epoxidation being the premier example.[5−8] On the biological front, there is ample evidence to support the involvement of oxygen atom transfer (OAT) in the reactions of dimethyl sulfoxide (DMSO) reductase, sulfite oxidase, and nitrate reductase.[4,9−11] In the active site of these enzymes, molybdenum cycles between Mo^{IV}, d^2, and Mo^{VI}, d^0, which are isoelectronic to Re^V and Re^{VII}, respectively. Of particular interest to us is the sulfite oxidase family, where the reduced state contains a monooxomolybdenum(IV), $Mo^{IV}(O)$, and the oxidized enzyme a dioxomolybdenum(VI), $Mo^{VI}(O)_2$.[4,12,13] Many model studies have employed DMSO in the oxidation of $Mo^{IV}(O)$ complexes and organic phosphanes in the reduction of $Mo^{VI}(O)_2$, Scheme 1.[14−17] Most of the known molybdenum model systems either are ineffective catalysts for OAT reactions or display sluggish kinetics. In addition, the formation of binuclear Mo^V, eq 2, intervenes with catalysis. However, a number of rhenium catalysts have been shown to transfer an oxygen atom efficiently from a sulfoxide to an appropriate oxygen acceptor such as triphenylphosphine,[18−20] hypophosphorus acid,[21] sulfides,[22−24] thiols,[25,26] and disulfides.[25] Even though some of the rhenium-

† Tel: (310) 206-2602. Fax: (310) 206-9130. E-mail: mao@chem.ucla.edu.

(1) Sheldon, R. A.; Kochi, J. K. *Metal-Catalyzed Oxidations of Organic Compounds*; Academic: New York, 1981.
(2) Owens, G. S.; Arias, J.; Abu-Omar, M. M. *Catal. Today* **2000**, *55*, 317−363.
(3) Collman, J. P.; Zhang, X.; Lee, V. J.; Uffelman, E. S.; Branman, J. I. *Science* **1993**, *261*, 1404−1411.
(4) Hille, R. *Chem. Rev.* **1996**, *96*, 2757−2816.
(5) Johnson, R. A.; Sharpless, K. B. In *Catalytic Asymmetric Synthesis*; Ojima, I., Ed.; VCH: New York, 1993, Chapter 4.1.
(6) Jacobsen, E. N. In *Catalytic Asymmetric Synthesis*; Ojima, I., Ed.; VCH: New York, 1993; pp 159−202.
(7) Jorgensen, K. A. *Chem. Rev.* **1989**, *89*, 431−458.
(8) Ito, Y. N.; Katsuki, T. *Bull. Chem. Soc. Jpn.* **1999**, *72*, 603−619.
(9) Schultz, B. E.; Hille, R.; Holm, R. H. *J. Am. Chem. Soc.* **1995**, *117*, 827−828.
(10) Enemark, J. H.; Young, C. G. *Adv. Inorg. Chem.* **1993**, *40*, 1−88.
(11) Young, C. G. In *Biomimetic Oxidations Catalyzed by Transition Metal Complexes*; Meunier, B., Ed.; Imperial College Press: London, 2000; pp 415−459.
(12) McMaster, J.; Enemark, J. H. *Curr. Opin. Chem. Biol.* **1998**, *2*, 201−207.
(13) Raitsimring, A. M.; Pacheco, A.; Enemark, J. H. *J. Am. Chem. Soc.* **1998**, *120*, 11263−11278.
(14) Caradonna, J. P.; Reddy, P. R.; Holm, R. H. *J. Am. Chem. Soc.* **1988**, *110*, 2139−2144.
(15) Schultz, B. E.; Holm, R. H. *Inorg. Chem.* **1993**, *32*, 4244−4248.
(16) Laughlin, L. J.; Young, C. G. *Inorg. Chem.* **1996**, *35*, 1050−1058.
(17) Xiao, Z.; Bruck, M. A.; Enemark, J. H.; Young, C. G.; Wedd, A. G. *Inorg. Chem.* **1996**, *35*, 7508−7515.
(18) Takacs, J.; Cook, M. R.; Kiprof, P.; Kuchler, J. G.; Herrmann, W. A. *Organometallics* **1991**, *10*, 316−320.
(19) Zhu, Z.; Espenson, J. H. *J. Mol. Catal. A* **1995**, *103*, 87−94.
(20) Arterburn, J. B.; Perry, M. C. *Tetrahedron Lett.* **1996**, *37*, 7941−7944.
(21) Abu-Omar, M. M.; Appleman, E. H.; Espenson, J. H. *Inorg. Chem.* **1996**, *35*, 7751−7757.
(22) Arterburn, J. B.; Nelson, S. L. *J. Org. Chem.* **1996**, *61*, 2260−2261.
(23) Brown, S. N.; Mayer, J. M. *J. Am. Chem. Soc.* **1996**, *118*, 12119−12133.
(24) Gunaratne, H. Q. N.; McKervey, M. A.; Feutren, S.; Finlay, J.; Boyd, J. *Tetrahedron Lett.* **1998**, *39*, 5655−5658.
(25) Arterburn, J. B.; Perry, M. C.; Nelson, S. L.; Dibble, B. R.; Holguin, M. S. *J. Am. Chem. Soc.* **1997**, *119*, 9309−9310.

10.1021/ic000917z CCC: $20.00
Published on Web 03/28/2001

Scheme 1

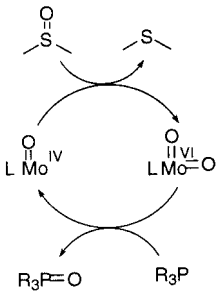

Scheme 2

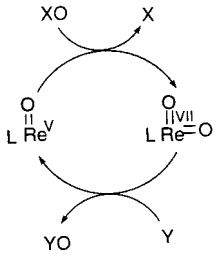

(V) catalysts act as Lewis acids,[26,27] others feature a metal-centered oxygen transfer (an oxotransferase) mechanism.[18,21,23] Thus, we anticipated that the oxidation of $Re^{V}(O)$ complexes by oxygen donors (such as sulfoxides or pyridine *N*-oxide) and the reduction of $Re^{VII}(O)_2$ by oxygen acceptors (such as sulfides), Scheme 2, should parallel the chemistry of molybdenum oxotransferases from a mechanistic standpoint while bypassing the kinetic inertness inherent in molybdenum coordination complexes.

$$[M]^n + XO \underset{k_r}{\overset{k_f}{\rightleftharpoons}} [M{=}O]^{(n+2)} + X \qquad (1)$$

$$LMo^{IV}(O) + LMo^{VI}(O)_2 \xrightarrow{k_d} L(O)Mo^{V}{-}O{-}Mo^{V}(O)L \qquad (2)$$

In this report, we detail the use of a new class of oxorhenium(V) catalysts in oxygen-transfer reactions with sulfoxides. The featured complex, bis[2-(2′-hydroxyphenyl)-2-oxazolinato]oxorhenium(V) trifluoromethanesulfonate, is a catalyst for the oxidation of sulfides and sulfoxides. A variety of reagents are known to effect the oxidation of sulfides to sulfoxides[28] and sulfoxides to sulfones.[29] OAT from aryl sulfoxides to alkyl sulfides and sulfoxides as catalyzed by oxorhenium(V) oxazoline complexes will be highlighted. A detailed mechanism for the catalytic reactions will be presented based on extensive kinetics and electronic studies. Our mechanistic findings reported herein will be related to the molybdenum-dependent oxotransferases.

Experimental Section

Chemicals and Instrumentation. All solvents were either HPLC or spectrophotometric grade and used as received unless specified otherwise. The ligand 2-(2′-hydroxyphenyl)-2-oxazoline[30] and the rhenium complex $Re(O)Cl_3(OPPh_3)(Me_2S)$[31] were prepared according to previous literature methods.

NMR spectra were obtained on Bruker AC200 and ARX400 spectrometers. UV−vis spectra were recorded on a Shimadzu UV-2501 spectrophotometer. Stopped-flow kinetics were collected on an Applied Photophysics SX.18MV stopped-flow reaction analyzer. Time profiles were analyzed with KaleidaGraph 3.0 on a Macintosh or PC.

Kinetics Studies. All UV−vis time profiles were performed in methylene chloride using quartz cells of 1.0 mm optical path length at 23.0 ± 0.5 °C. The formation of aryl sulfide products was monitored at 260 nm. Extinction coefficients (ϵ) of aryl sulfides in the UV are about 4 times those of aryl sulfoxides.[32] The kinetics of sulfoxide oxidation was followed by ^{1}H NMR in CD_3CN, and initial rates were computed over ∼10% conversion. Unless specified otherwise, all reactions proceeded to completion and percent yields were determined by ^{1}H NMR. Stock solutions of the oxorhenium(V) catalysts were prepared in either methylene chloride or acetonitrile and stored at −20 °C.

Synthesis of Chlorobis[2-(2′-hydroxyphenyl)-2-oxazolinato]oxorhenium(V), $(hoz)_2Re(O)Cl$, 1. To 0.51 g (0.79 mmol) of $Re(O)Cl_3(OPPh_3)(Me_2S)$ in 100 mL of absolute ethanol was added 0.28 g (1.74 mmol) of free ligand 2-(2′-hydroxyphenyl)-2-oxazoline. The solution was refluxed under argon for 4 h, cooled to room temperature, and filtered, yielding a green solid, which was washed with 3 × 5 mL portions of cold ether and one portion of ethanol. Recrystallization from a 1:1 mixture of dichloromethane and pentane gave 0.23 g (49% yield) of complex **1**. FT-IR (Nujol) in cm^{-1}: 973 (Re═O), 1630 (C═N), 1606, 1586, 1544. ^{1}H NMR (400 MHz) in CD_2Cl_2: δ 4.17−4.26 (m, 2H), 4.72 (m, 2H), 4.87−5.07 (m, 4H), 6.74−6.97 (m, 4H), 7.25 (t, 1H), 7.46 (t, 1H), 7.68 (d, 1H), 7.94 (d, 1H). EI/MS: m/z = 527 (MOL_2^+), and 562 (MOL_2Cl^+) with correct rhenium 187/185 and chlorine 37/35 isotope ratios.

Synthesis of Bis[2-(2′-hydroxyphenyl)-2-oxazolinato]aquo-oxorhenium(V) Trifluoromethanesulfonate, $[(hoz)_2Re(O)(OH_2)][OTf]$, 2. To 92 mg (0.16 mmol) of complex **1** in 50 mL of CH_3CN was added 62 mg (0.24 mmol) of silver triflate. After 4 h of refluxing, the white AgCl which precipitated from the olive green solution was filtered off, and the supernatant was evaporated, yielding 100 mg (95%) of dark green crystals. FT-IR (Nujol) in cm^{-1}: 984 (Re═O), 1643 (C═N), 1580, 1538. ^{1}H NMR (400 MHz) in acetonitrile-d_3: δ 4.33 (q 8.00 Hz, 2H), 4.60 (q 11.51 Hz, 2H), 4.99 (q 9.60 Hz, 2H), 5.13 (q 7.59 Hz, 2H), 7.02 (d 8.21 Hz, 2H), 7.08 (t 8.00 Hz, 2H), 7.57 (t 7.20 Hz, 2), 7.91 (d 7.38 Hz, 2H). ^{19}F NMR (400 MHz) in acetonitrile-d_3: δ −79.86. EI/MS: m/z = 527 (MOL_2^+), and 676 (MOL_2OTf^+) with correct rhenium 187/185 isotope ratios.

X-ray Structure Determination of $[(hoz)_2Re(O)(OH_2)][OTf]$, 2. A green crystal of catalyst **2** was grown by slow evaporation of a methylene chloride solution at −10 °C. A suitable crystal of approximate dimensions 0.35 × 0.25 × 0.15 mm was mounted on a glass fiber. X-ray intensity data were collected at 123(2) K on a modified Picker diffractometer with graphite-monochromated Mo Kα radiation. Crystallographic data are summarized in Table 1. The crystal was triclinic (space group $P\bar{1}$). The unit cell was determined on the basis of 7807 reflections with 1.47° < θ < 25.00°. Crystal quality was monitored by recording three standard reflections approximately every 97 reflections measured; no significant variation in intensity was shown. Reflection data were corrected for Lorentz and polarization effects. A semiempirical absorption correction was carried out using ψ scans. The structure was solved by Patterson and Fourier techniques. All non-hydrogen atoms were calculated at idealized positions and were included in refinement as fixed contributors. The final difference Fourier map was featureless, the largest peak (1.941 e/Å^3) being adjacent to a rhenium atom.

In situ Preparation of Bis[2-(2′-hydroxyphenyl)-2-oxazolinato]-dioxorhenium(VII) Trifluoromethanesulfonate, $[(hoz)_2Re(O)_2][OTf]$,

(26) Abu-Omar, M. M.; Khan, S. I. *Inorg. Chem.* **1998**, *37*, 4979−4985.
(27) Conry, R. R.; Mayer, J. M. *Inorg. Chem.* **1990**, *29*, 4862−4867.
(28) Reagents that oxidize sulfides to sulfoxides: 1 equiv of 30% H_2O_2, ^{t}BuOOH, $NaClO_2$, NaOCl, dioxiranes, HNO_3 and an $AuCl_4^-$ catalyst, and peracids. March, J. *Advanced Organic Chemistry: Reactions, Mechanisms, and Structure*, 4th ed.; Wiley: New York, 1992; pp 1201−1203.
(29) Reagents that oxidize sulfoxides to sulfones: $KMnO_4$, sodium perborate, $KHSO_5$. March, J. *Advanced Organic Chemistry: Reactions, Mechanisms, and Structure*, 4th ed.; Wiley: New York, 1992; pp 1201−1203.
(30) Hoveyda, H. R.; Rettig, S. J.; Orvig, C. *Inorg. Chem.* **1992**, *31*, 5408−5416.
(31) Grove, D. E.; Wilkinson, G. *J. Chem. Soc. A* **1966**, 1224−1230.
(32) Vassell, K. A.; Espenson, J. H. *Inorg. Chem.* **1994**, *33*, 5491−5498.

Table 1. Crystallographic Data and Structure Refinement for $[(hoz)_2Re(O)(OH_2)][OTf]$, **2**

empirical formula	$C_{19}H_{18}F_3N_2O_9ReS$
fw	693.61
temp, K	123(2)
λ (Å)	0.71073 (Mo Kα)
cryst syst	triclinic
space group	$P\bar{1}$
reflns collected	7807
indep reflns	7807 [R(int) = 0.0000]
a, Å	13.61(2)
b, Å	14.76(2)
c, Å	11.871(14)
α, deg	93.69(4)
β, deg	99.43(4)
γ, deg	108.44(4)
Z	4
V, Å^3	2213(5)
ρ(calcd), g cm^{-3}	2.082
μ, mm^{-1}	5.666
F(000), e	1344
θ range, deg	1.47−25.00
cryst size, mm	0.35 × 0.25 × 0.15
abs correction	empirical
max. and min. transm	1.00 and 0.66
refinement meth	full-matrix least-squares of F^2
data/restraints/params	7807/0/631
GOF on F^2	1.038
R indices [$I > 2\sigma(I)$][a]	R1 = 0.0455, wR2 = 0.1055
R indices (all data)[a]	R1 = 0.0786, wR2 = 0.1230

[a] $R1 = \sum||F_o| - |F_c||/\sum|F_o|$, $wR2 = (\sum w(|F_o| - |F_c|)^2/\sum w|F_o|^2)^{1/2}$.

3. To 9 mg (13 μmol) of catalyst **2** in 0.6 mL of CD_3CN was added 3 mg (28 μmol) of 4-picoline *N*-oxide. The solution turned almost instantly from green to red/brown. In rigorously dried solvent, **3** is stable for days at −10 °C. ^{1}H NMR (200 MHz) in CD_3CN: δ 4.20 (t, 2H), 4.66 (t, 2H), 4.96−5.06 (m, 4H), 7.02−7.23 (m, 4H), 7.48 (t, 1H), 7.72 (t, 1H), 7.88 (d, 1H), 7.92 (d, 1H). FAB/MS (NBA-matrix): m/z = 543 ($MO_2L_2^+$), 527 (MOL_2^+), and 381 (MO_2L^+) with correct rhenium 187/185 isotope ratios.

Stopped-Flow Kinetics with 3 under Non-Steady-State Conditions. Solutions of the dioxorhenium(VII) complex **3** were prepared by adding a stoichiometric amount of 4-picoline *N*-oxide (5.0×10^{-4} M) to **2** (5.0×10^{-4} M) in acetonitrile at 25 °C. The reaction was followed to completion by UV−vis at 500 nm, where **3** absorbs exclusively.[33] Solutions of **3** prepared in this way were used within 1 h of preparation, even though only slight decomposition was detected after several hours. The dioxorhenium(VII) was then reduced in situ with excess substituted thioanisole, $(XC_6H_4)SCH_3$ (4.0×10^{-3} to 0.090 M), to achieve pseudo-first-order conditions; the decay of the absorbance at 500 nm was monitored by stopped-flow. Plots of the pseudo-first-order rate constants (k_ψ) versus $[(XC_6H_4)SCH_3]$ were linear, and their slopes afforded second-order rate constants for the different derivatives of thioanisole.

Results

X-ray Molecular Structure of $[(hoz)_2Re(O)(H_2O)][OTf]$, 2. The single-crystal X-ray structure of **2** contains isolated molecules with octahedral geometry about the rhenium, Figure 1. Although the complex shows no signs of decomposition when exposed to air and moisture, it is hygroscopic; thus, the X-ray data contains a water molecule in place of the weakly coordinating triflate anion. The phenoxide oxygens bind trans with respect to each other, as do the oxazoline nitrogens. This is in contrast to the chloride precursor complex **1** in which the phenoxide oxygens bind cis to each other. An X-ray structure of **1** was not taken because all other spectroscopic data is consistent with the bromide analogue, $(hoz)_2Re(O)Br$, which has been structurally characterized.[34]

Two independent molecules with virtually identical parameters are present in the asymmetric unit cell. The Re=O distance of 1.679(7) Å is typical for monooxo rhenium(V) complexes.[35] The observed Re−O distance for the bound water is 2.272(7) Å, which is in the range observed for other aquo rhenium complexes.[36,37] Crystallographic tables containing (1) positional and equivalent isotropic thermal parameters, (2) bond lengths, and (3) bond angles are provided in the Supporting Information.

Oxidation of Sulfides with Sulfoxides. Complexes **1** and **2** catalyze the oxidation of alkyl sulfides with aryl sulfoxides, eq 3. The progress of the reaction was followed at 260 nm, where the aryl sulfide product absorbs. Kinetics were collected using catalytic amounts of rhenium, excess alkyl sulfide, and limiting aryl sulfoxide. Under these conditions, the data fits pseudo-first-order kinetics, eq 4. Two representative time-profiles are shown in Figure S1 for the formation of diphenyl sulfide from the oxidation of dimethyl sulfide by diphenyl sulfoxide. As evident from Figure S1 (Supporting Information), catalyst **1** is less reactive than catalyst **2**, Table 2. This observation is consistent with a mechanism in which an open coordination site on the catalyst is required. The dependence of the kinetics on the oxidizing sulfoxide was probed for both catalysts **1** and **2**, Table 2. For both catalysts an electron-donating substituent (a methyl in place of a phenyl) increases the reaction rate. PhS(O)Me is a better nucleophile than Ph_2SO, and, thus, it is a better ligand for rhenium. The sulfoxide coordinates to rhenium via oxygen, followed by an oxygen-transfer reaction producing dioxorhenium(VII) and sulfide.

$$PhS(O)R' + R_2S \xrightarrow{Re^{V}\ cat.} PhSR' + R_2SO \qquad (3)$$

(R′ = Ph or Me and R = alkyl)

$$Abs_t = Abs_\infty + \{Abs_0 - Abs_\infty\}e^{-k_\psi t} \qquad (4)$$

Since **2** is clearly the superior catalyst, henceforth it was employed in all the kinetics investigations. The reaction rate for the oxidation of dimethyl sulfide with diphenyl sulfoxide showed first-order dependence on $[Ph_2SO]$ and catalyst, Figure S2 (Supporting Information). However, the dependence on dimethyl sulfide was more conglomerate. The rate increases to a maximum as sulfide concentration increases and declines at yet higher sulfide concentrations. In order to further investigate this unusual dependence on dimethyl sulfide, we employed bulkier alkyl sulfides, namely, diethyl and di-*tert*-butyl sulfides, Figure 2. Initial rate method was utilized to avoid mixed second-order kinetics at lower sulfide concentrations. The inhibition by substrate is less pronounced as the bulkiness of the R group increases from Me to ^{t}Bu. These findings are consistent with a mechanism in which the sulfide competes for coordination on the rhenium with diphenyl sulfoxide, Scheme 3. The steady-state rate law for the mechanism in Scheme 3 is shown in eq 5. Since Ph_2SO was the limiting reagent and initial rates were measured prior to significant formation of Ph_2S, the terms with $[Ph_2S]$ in the denominator of eq 5 drop out, and the rate law simplifies to that in eq 6. Nonlinear-least-squares fitting of the

(33) Abu-Omar, M. M.; McPherson, L. D.; Arias, J.; Béreau, V. M. *Angew. Chem., Int. Ed.* **2000**, *39*, 4310−4313.
(34) Shuter, E.; Hoveyda, H. R.; Karunaratne, V.; Rettig, S. J.; Orvig, C. *Inorg. Chem.* **1996**, *35*, 368−372.
(35) Nugent, W. A.; Mayer, J. M. *Metal-Ligand Multiple Bonds*; Wiley Interscience: New York, 1988; pp 175−176.
(36) Ciani, G.; Giusto, D.; Manassero, M.; Sansoni, M. *J. Chem. Soc., Dalton Trans.* **1975**, 2156−2161.
(37) Muller, U. *Acta Crystallogr. (C)* **1984**, *40*, 571−572.

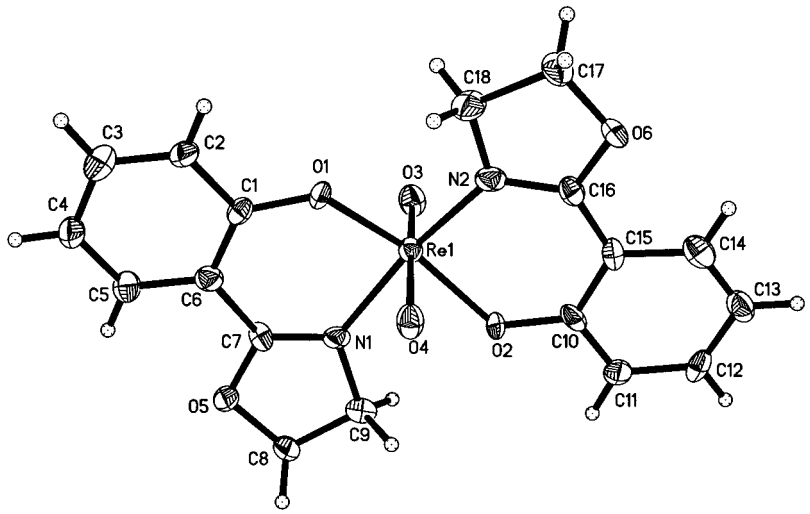

Figure 1. ORTEP molecular structure representation of $[(hoz)_2Re(O)(OH_2)][OTf]$, **2**. The triflate counterion is not shown. Selected bond distances (Å) and angles (deg): Re(1)−O(3) = 1.679(7), Re(1)−O(2) = 1.983(7), Re(1)−O(1) = 1.987(7), Re(1)−O(4) = 2.272(7), Re(1)−N(1) = 2.035(8), Re(1)−N(2) = 2.064(8), O(3)−Re(1)−O(4) = 178.3(3), O(2)−Re(1)−O(3) = 100.4(3), O(3)−Re(1)−N(1) = 101.1(3), O(4)−Re(1)−O(1) = 79.0(3), N(2)−Re(1)−O(4) = 79.7(3).

Table 2. Rate of Oxygen Atom Transfer to Me_2S as a Function of Catalyst and Oxidant (Eq 3)[a]

PhS(O)R′	Re(V) cat.	k_ψ/s^{-1}
PhS(O)Ph	**1**	$(9.2 \pm 0.2) \times 10^{-5}$
PhS(O)Me	**1**	$(6.2 \pm 0.7) \times 10^{-4}$
PhS(O)Ph	**2**	1.8×10^{-3} [b]
PhS(O)Me	**2**	6.7×10^{-3} [b]

[a] Conditions: $[PhS(O)R'] = 1.0 \times 10^{-3}$ M, $[Me_2S] = 2.0 \times 10^{-2}$ M, $[Re] = 2.0 \times 10^{-4}$ M in CH_2Cl_2 at 23 °C. [b] Errors in exponential fit are negligible ($<1 \times 10^{-5}$).

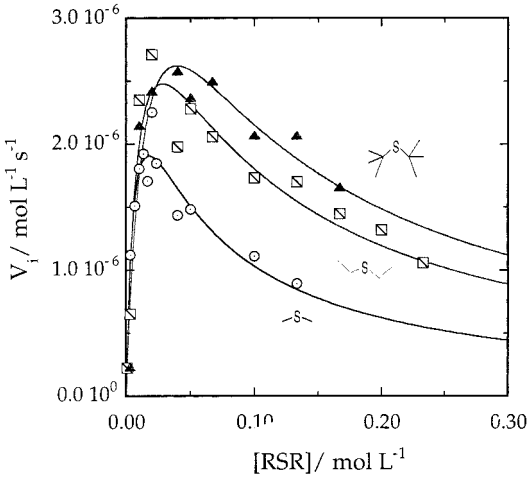

Figure 2. Plot of V_i versus [RSR] for Me_2S (circles), Et_2S (squares), and ^{t}BuS (triangles) illustrating the effects of steric hindrance on the reducing sulfide. Conditions: $[RSR] = 1.3 \times 10^{-3}$ to 2.3×10^{-1} M, $[Ph_2SO] = 1.2 \times 10^{-3}$ M, [**2**] $= 1.8 \times 10^{-4}$ M in CH_2Cl_2 at 23 °C and 1.0 mm optical path length. The solid lines are nonlinear least-squares regressions for eq 6, and the determined rate constants are summarized in Table 3.

initial-rate data to eq 6 (Figure 2) yields the constants k_1, K_2, and k_3 for the different alkyl sulfides, Table 3. It is worth noting that, within experimental error, the different substrates give the same k_1 value, which is characterized by Ph_2SO and not R_2S, Scheme 3. Furthermore, K_2 is dependent on the alkyl sulfide and decreases as the steric hindrance increases; ^{t}Bu$_2$S is a worse ligand than Me_2S. Perhaps most surprising is the mild steric sensitivity displayed by the oxidation step, k_3, in Scheme 3. The oxo ligands of complex **3** are readily accessible to the substrate such that Me_2S is slightly more reactive than ^{t}Bu$_2$S.

$$\frac{d[Ph_2S]}{dt} = \{k_1k_{-2}k_3[Ph_2SO][R_2S][Re]_T\}/\{k_{-2}k_1[Ph_2SO] + k_{-1}k_{-2}[Ph_2S] + k_{-1}k_2[R_2S][Ph_2S] + k_3k_{-2}[R_2S] + k_3k_2[R_2S]^2\} \quad (5)$$

$$\frac{d[Ph_2S]}{dt} = \{k_1[Ph_2SO][R_2S][Re]_T\}/\{(k_1/k_3)[Ph_2SO] + [R_2S] + K_2[R_2S]^2\} \quad (6)$$

Thermodynamics of Oxygen Atom Transfer. According to gas-phase data, aryl sulfoxide S═O bonds are stronger than alkyl ones by 1−3 kcal mol^{-1}.[38,39] In other words, the reaction described in eq 3 should be favored in the opposite direction to what was observed in this study. However, it is a well-known fact that gas-phase data should be applied to solution studies with caution. Thus, we were prompted to determine the thermodynamics for a couple of reactions from equilibrium measurements in solution employing catalyst **2**. Via ^{1}H NMR, the equilibrium constants for reactions 7 and 8 were evaluated in CD_3CN at 25 °C to be 140 and 24, respectively. Typical conditions for the NMR equilibrium studies were as follows: $[Ph_2SO] = 0.30$ M, $[Me_2S]$ or $[PhSMe] = 0.30$ M, and [**2**] $= 7.4 \times 10^{-3}$ M. These equilibrium values translate into $\Delta G°$ of −2.9 kcal mol^{-1} for reaction 7 and −1.9 kcal mol^{-1} for reaction 8. This is in sharp contrast to the gas-phase data of +3 and +1 kcal mol^{-1} for reactions 7 and 8, respectively.[39] Therefore, in solution aryl sulfoxides are better oxidants than their alkyl counterparts.

		$\Delta G°$/kcal mol^{-1}	
		this work	gas phase[39]
$Ph_2SO + Me_2S \rightleftarrows Ph_2S + Me_2SO$	(7)	−2.9	+3.0
$Ph_2SO + PhSMe \rightleftarrows Ph_2S + PhS(O)Me$	(8)	−1.9	+1.0

From the reactions that **2** is capable of catalyzing (eqs 3, 7, and 8), the thermodynamics of the Re^V/Re^{VII} couple in CH_3CN

(38) Jenks, W. S.; Matsunaga, N.; Gordon, M. *J. Org. Chem.* **1996**, *61*, 1275−1283.
(39) Holm, R. H.; Donahue, J. P. *Polyhedron* **1993**, *12*, 571−589.

Scheme 3

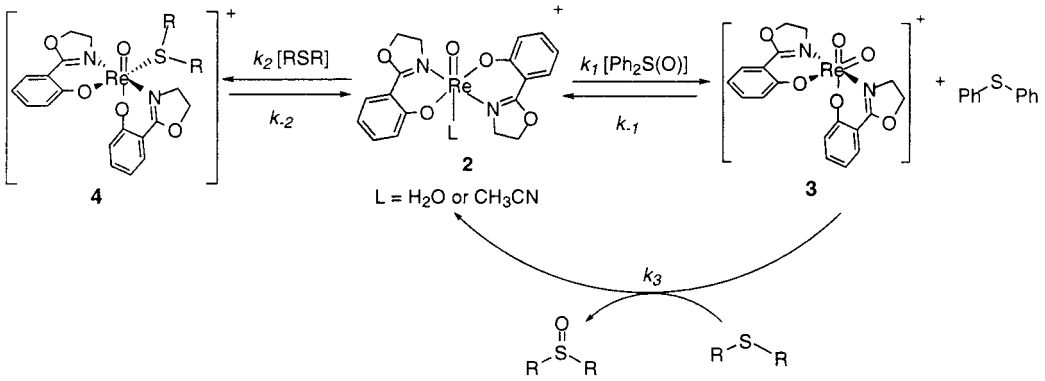

Table 3. Rate Constants for the Oxidation of Several Alkyl Sulfides with Ph_2SO as Catalyzed by **2** (Scheme 3 and Eq 6)

RSR	k_1/ L mol^{-1} s^{-1}	K_2/ L mol^{-1}	k_3/ L mol^{-1} s^{-1}
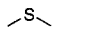	16 ± 3	22 ± 3	3.0 ± 0.5
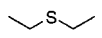	20 ± 4	14 ± 2	2.5 ± 0.4
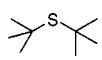	21 ± 4	8 ± 2	1.7 ± 0.3

can be estimated, eq 9. The cationic dioxorhenium(VII) oxazoline complex, **3**, is a comparable oxidant to the chromyl ion[40] ($CrO^{2+}_{(aq)} \rightarrow Cr^{2+}_{(aq)} + {}^1/_2O_{2(g)}$, $\Delta G° = 23$ kcal mol^{-1}), and the Re^{VII}=O bond strength in **3** is weaker than that of vanadyl[41] and methyltrioxorhenium (MTO):[21] $VO^{2+}_{(aq)} \rightarrow V^{2+}_{(aq)} + {}^1/_2O_{2(g)}$, $\Delta G° = 55$ kcal mol^{-1}; $CH_3ReO_{3(aq)} \rightarrow CH_3ReO_{2(aq)} + {}^1/_2O_{2(g)}$, $\Delta G° = 56$ kcal mol^{-1}.

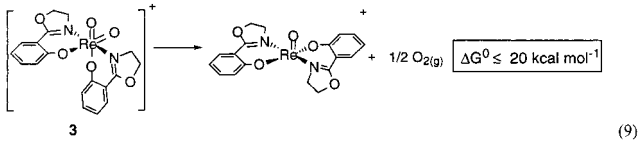

(9)

The Dioxorhenium(VII) Intermediate. Even though under steady-state conditions the majority of the catalyst is present in the +5 oxidation state as complex **2**, addition of oxygen donors in the absence of a reductant gives the cationic dioxorhenium(VII) complex **3**. Typical oxygen donors include pyridine *N*-oxide, aqueous hydrogen peroxide, and ^{t}BuOOH. Recently we have reported on the reduction of perchlorate ions with compounds **1** and **2**, which also proceeds via dioxorhenium(VII).[33] The UV−vis spectrum of **2** features only a weak d−d transition in the visible region ($\lambda_{max} = 570$ nm, $\epsilon = 118$ L mol^{-1} cm^{-1}). Upon addition of an oxygen donor (Py-*N*-O, H_2O_2, or ^{t}BuOOH), an intense band grows at 500 nm ($\epsilon = 1275$ L mol^{-1} cm^{-1}).[33] On visual inspection, solutions of **2** turn from green to red/brown upon addition of an oxygen donor. Complex **3** was also characterized by NMR and mass spectrometry (see Experimental Section). The ^{1}H NMR spectrum shows two different oxazoline ligand environments, which is consistent with the expected cis dioxo geometry for a d^0 center.

When sulfoxides are used as the oxygen donor, the equilibrium lies in favor of rhenium(V), complex **2**. Thus, even in the absence of a reductant, sulfoxides do not give a detectable amount of complex **3**, and the solution stays green in color. The exception thus far has been diphenyl sulfoxide, which produces detectable amounts of **3**. Therefore, it is a reasonable extrapolation to propose that oxygen-transfer reactions with sulfoxides proceed via complex **3**.

In the absence of water, complex **3** is long-lived. For example, when 4-picoline *N*-oxide is used in dry acetonitrile, solutions of **3** persist for days at −10 °C without sign of degradation. Water hydrolyzes **3** to **5**, eq 10.[33] Complex **5** has been prepared independently from the reaction of $ClReO_3$[42] and the sodium salt of the oxazoline ligand (made by the action of NaH on the parent ligand). Complex **5** was characterized spectroscopically: ^{1}H NMR in $CDCl_3$, δ 4.96 (t, 2H), 5.01 (t, 2H), 7.01−7.21 (m, 2H), 7.72 (t, 1H), 7.87 (d, 1H); EI/MS, $m/z = 397$ (MO_3L^+). The neutral trioxorhenium(VII) complex is inactive as an oxygen-transfer catalyst; it oxidizes neither dimethyl sulfide nor phosphanes. Triphenylphosphine merely coordinates to complex **5**, eq 11: ^{31}P NMR, −3.7 ppm.

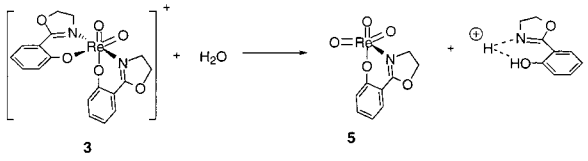

(10)

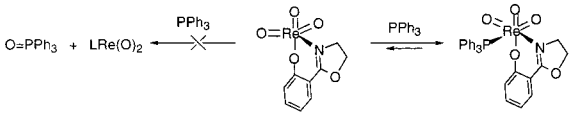

(11)

Sulfoxide Disproportionation and Oxidation. Even though the disproportionation of sulfoxides is energetically very favorable ($2Me_2SO$ == $Me_2S(O)_2 + Me_2S$, $\Delta G° = -25$ kcal mol^{-1}),[39] the process is prevented by extremely slow kinetics, a fact which makes sulfoxides stable indefinitely. Complex **2** catalyzes the disproportionation of sulfoxides to sulfone and sulfide under ambient conditions. Also the oxidation of alkyl sulfoxides by aryl sulfoxides is catalyzed by **2** selectively as illustrated in eq 12. The rate of oxidation of sulfoxides to sulfones by **3** is orders of magnitude slower than that of sulfides to sulfoxides; thus, in the presence of sulfide, sulfoxides are exclusively produced (vide supra).

$$PhS(O)R' + Me_2SO \xrightarrow{\text{cat. } 2} PhSR' + Me_2S(O)_2 \quad (12)$$

$$(R' = Ph \text{ or } Me)$$

The kinetics of sulfoxide oxidation are first-order in $[Re]_T$ and each of the sulfoxide reactants. The sulfide product inhibits

(40) Scott, S. L.; Bakac, A.; Espenson, J. H. *J. Am. Chem. Soc.* **1992**, *114*, 4205−4213.
(41) The NBS Tables of Chemical Thermodynamic Properties. *J. Phys. Chem. Ref. Data* **1982**, *11*, Suppl. No. 2.

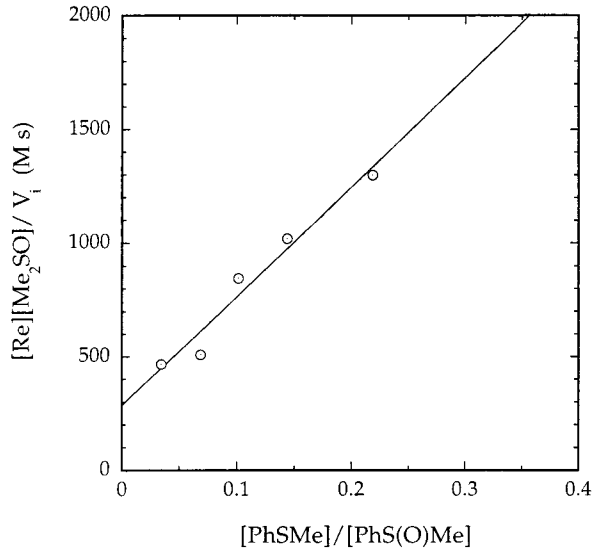

Figure 3. Plot of $[Re]_T[Me_2SO]/V_i$ versus [PhSMe]/[PhS(O)Me] for the oxidation of DMSO catalyzed by **2**. The data is fit to the rate law in eq 14; see text and Table 4 for conditions and results.

Scheme 4

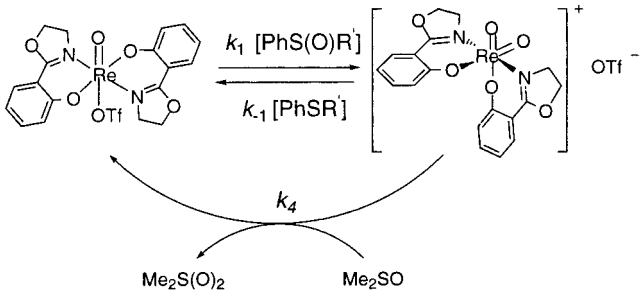

the reaction. These observations are in agreement with the mechanism in Scheme 4 and its corresponding rate law in eq 13. Since sulfoxides are much less reactive than sulfides, the formation of complex **3** is rapid relative to oxygen atom transfer to sulfoxide, i.e., $k_1[PhS(O)R'] + k_{-1}[PhSR'] \gg k_4[Me_2SO]$. In other words, the rate law simplifies to the prior equilibrium limit, which gives eq 14 after rearrangement. Measurements of the initial rate by ^1H NMR at different ratios of [PhSMe]/[PhS(O)Me] and constant $[Me_2SO]$ and $[Re]_T$ conforms to eq 14, Figure 3. Similar kinetic behavior is observed for the disproportionation of sulfoxide in which the sulfoxide dependence is second order. Unfortunately, the high uncertainty in the intercept of eq 14 stifles the determination of k_4 with precision; thus, the treatment is limited to yielding the combination of K_1k_4, Table 4.

$$\frac{d[MeS(O)_2Me]}{dt} = \frac{k_4k_1[PhS(O)R'][Me_2SO][Re]_T}{k_{-1}[PhSR'] + k_1[PhS(O)R'] + k_4[Me_2SO]} \quad (13)$$

$$\frac{[Me_2SO][Re]_T}{V_i} = \frac{1}{K_1k_4}\frac{[PhSR']}{[PhS(O)R']} + \frac{1}{k_4} \quad (14)$$

It is worth noting from Table 4 that $k_4(Me_2SO)/k_4(PhS(O)Me) = 1.8$ when Ph_2SO is the oxidant (entries 1 and 2), and $k_4(Me_2SO)/k_4(PhS(O)Me) = 2.1$ when PhS(O)Me is the oxidant (entries 3 and 4). This trend is in agreement with a common oxidizing intermediate (complex **3**) irrespective of the stoichiometric sulfoxide oxidant. The reactivity trend also points to the reducing sulfoxide as the nucleophile in its reaction with dioxorhenium(VII). Furthermore, the equilibrium constant K_1 is larger for Ph_2SO than PhS(O)Me, $K_1(PhS(O)Ph)/K_1(PhS(O)Me) = 34$ with Me_2SO as the reductant (entries 1 and 3), and $K_1(PhS(O)Ph)/K_1(PhS(O)Me) = 40$ with PhS(O)Me as the reductant (entries 2 and 4). In other words, the formation of dioxorhenium(VII) **3** is more favored thermodynamically with Ph_2SO than with PhS(O)Me (vida supra).

Table 4. Rate Constants for the Oxidation and Disproportionation of Sulfoxides[a]

entry	oxidant	reductant	products	K_1k_4/L mol^{-1} s^{-1}
1	Ph_2SO	Me_2SO	$Ph_2S/Me_2S(O)_2$	$(7.1 \pm 4.9) \times 10^{-3}$
2	Ph_2SO	PhS(O)Me	$Ph_2S/PhS(O)_2Me$	$(4.0 \pm 0.6) \times 10^{-3}$
3	PhS(O)Me	Me_2SO	$PhSMe/Me_2S(O)_2$	$(2.1 \pm 0.1) \times 10^{-4}$
4	PhS(O)Me	PhS(O)Me	$PhSMe/PhS(O)_2Me$	$(1.0 \pm 0.3) \times 10^{-4}$
5	Me_2SO	Me_2SO	$Me_2S/Me_2S(O)_2$	nd[b]

[a] Conditions: $[Re]_T = 6.0-10.0$ mM (entries 1−4), [(product) sulfide] = 0.0040−0.080 M (entries 1−4), $[Ph_2SO] = 0.14$ M with either [PhS(O)Me] or $[Me_2SO] = 0.040$ M in CD_3CN at 23 °C (entries 1 and 2), [PhS(O)Me] = 0.14 M with $[Me_2SO] = 0.070$ M in CD_3CN at 23 °C (entry 3), [PhS(O)Me] = 0.13 M in CD_3CN at 23 °C (entry 4), $[Re]_T = 4.9$ mM and $[Me_2SO] = 0.197$ M in $CDCl_3$ at 23 °C (entry 5). [b] Not determined, 22% disproportionation after several days.

Discussion

Two rhenium(V) oxo complexes featuring the anionic phenoxy-oxazoline ligand were synthesized by established methodologies from readily available starting reagents. The bromo analogue of **1** has been synthesized previously from $[n\text{-}Bu_4N][Re(O)Br_4]$, which is quite sensitive to moisture and difficult to obtain pure.[34] Our synthesis, on the other hand, employs *cis,mer*-$Re(O)Cl_3(Me_2S)(OPPh_3)$, which is stable toward air and moisture and gives higher yields. Metathesis of the chloride in complex **1** afforded the cationic oxorhenium(V) triflate, **2**, with a coordinated water trans to the oxo ligand. Cationic $Re^V{=}O$ complexes with tris(pyrazolyl)borate ligands have been proposed by Mayer's group in OAT processes, in phenyl migration from rhenium to the oxo ligand, and in the oxidation of alkoxide ligands to aldehydes.[23,43] Therefore, **2** is highly suited for catalyzing OAT reactions with biologically relevant substrates such as sulfoxides. The availability of a coordination site makes **2** more reactive than **1**. The catalytic chemistry of **2** can be accounted for by the few transformations shown in Scheme 3. Aryl sulfoxides donate an oxygen atom to rhenium(V), generating a cationic dioxorhenium(VII), **3**, as a steady-state intermediate. The reducing alkyl sulfide accepts an oxygen atom from **3**, releasing the sulfoxide product and restoring **2**. Complex **3** can be prepared in the absence of a reductant and by employing a conventional oxygen donor (XO) such as pyridine *N*-oxide. Even inorganic oxoanions such as NO_3^- and ClO_4^-, which are of biological and environmental interests, react via OAT with **2** to give complex **3**.[33] The physical, spectroscopic, and structural data are totally consistent with the proposed formulations.

The catalytic kinetics of sulfide oxidation with aryl sulfoxides display an unprecedented inhibition by the reducing alkyl sulfide. The mechanism of inhibition was scrutinized by varying the bulkiness of alkyl substituents on the organic sulfide. The kinetic data is entirely consistent with a competitive reaction in which the reducing sulfide coordinates to complex **2**, yielding

(42) Herrmann, W. A.; Kuhn, F. E.; Romao, C. C.; Kleine, M.; Mink, J. *Chem. Ber.* **1994**, *127*, 47−54.

(43) DuMez, D. D.; Mayer, J. M. *Inorg. Chem.* **1998**, *37*, 445−453.

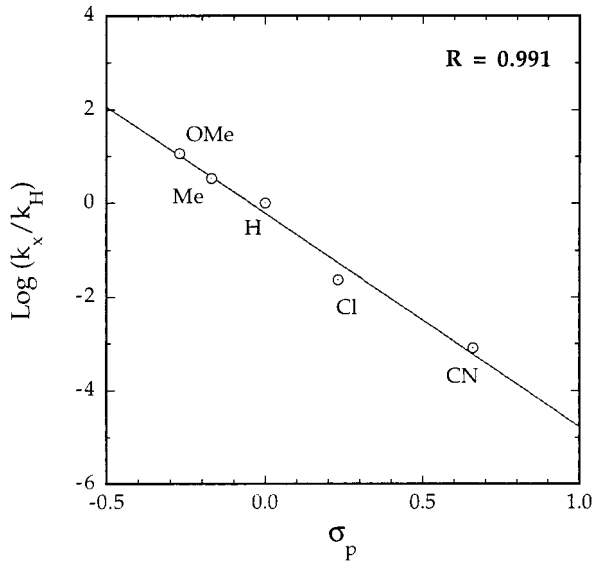

Figure 4. Hammett plot, $\log(k_x/k_H)$ vs σ_p, showing the electronic influences of para-substituted thioanisole derivatives on k_3. [**3**] = 5.0×10^{-4} M, [XC_6H_4SMe] = 3.8×10^{-3} to 8.9×10^{-2} M in CH_3CN at 25 °C.

an inactive sulfide adduct, **4**. The steady-state rate law for Scheme 3 is given in eq 5. A similar mechanism, Scheme 4, describes the experimental rate law (eq 14) observed for sulfoxide oxidation and disproportionation.

The active form of the catalyst, $[(hoz)_2Re(O)_2]^+$ (**3**), is stable for prolonged periods of time in the absence of moisture. Loss of catalytic activity is accounted for by the hydrolysis reaction of **3** to afford $(hoz)Re(O)_3$ (**5**). However, catalyst deactivation is insignificant under typical catalytic conditions, since the second-order rate constant for reaction 10 is 2.8×10^{-4} M^{-1} s^{-1}.[33] Three π-donating oxo ligands in **5** clearly enhance the stability of rhenium(VII), weakening its oxidizing ability. The charge on the rhenium complex might also be significant. Recently, Seymore and Brown showed large charge effects on the kinetics of oxygen-transfer reactions from Re^{V} complexes to phosphanes.[44] Inertness of trioxorhenium(VII) complexes has precedence in the literature; for example, methyltrioxorhenium-(VII),[2] $[(Me_3tacn)ReO_3]^+$,[27,45] and $[(HBpz_3)ReO_3]$[23,46] exhibit mild electrophilic oxo ligands, and thus do not oxidize sulfides.

Electronic Effects on Oxygen Atom Transfer to Sulfur. The oxidizing dioxorhenium(VII), **3**, possesses electrophilic oxo ligands. The observed trends in the rate of sulfide and sulfoxide oxidation are in support of this notion. In order to probe the electronic sensitivity of OAT from **3**, a few phenylmethyl sulfides with different substituents on the phenyl ring were studied under non-steady-state conditions. Substituents in the para position were employed to avoid interference from sterics. Insight into the nature of the transition state was sought from the structure−reactivity correlation of Hammett.[47,48] The rate constants for the oxidation of phenylmethyl sulfides were correlated with σ_p. Figure 4 shows a plot of $\log(k_X/k_H)$ versus σ; the slope corresponds to the reaction constant $\rho = -4.56 \pm 0.35$. The negative sign of ρ indicates a positive charge buildup on sulfur and agrees with the assigned mechanism in which the nucleophilic sulfide attacks the electrophilic oxygen on rhenium(VII). Therefore, we suggest the following structure for the transition state (a similar transition state could be drawn for sulfoxide oxidation to sulfone):

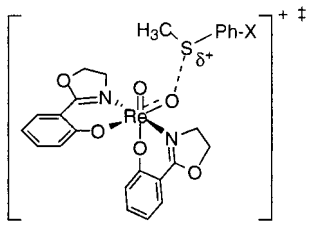

Once the oxygen atom is transferred from rhenium(VII) to the sulfide, the sulfoxide product is exchanged with a solvent molecule. This last step in the catalytic cycle could proceed via an associative (A) or dissociative (D) pathway. We favor the latter, since substitution reactions of **2** follow a D or I_d mechanism, and seven-coordinate oxorhenium(V) complexes are very rare.[33,49]

The large value of ρ (−4.6) indicates that the reaction is much more sensitive to electronic variations than benzoic acid, the reference substrate for the Hammett scale. This pronounced sensitivity to electronics is unusual and might be indicative of the high electrophilicity of the oxo ligands in complex **3**, which is probably comparable to that of $[(HBpz_3)Re(Ph)(O)_2][OTf]$.[23] Also, the charge on the dioxorhenium(VII) complex might in part be responsible for this conspicuous sensitivity to electronics.[44]

Our mechanistic findings parallel a theoretical study on the mechanism of OAT from $Mo(O)_2(NH_3)_2(SH)_2$ to PMe_3.[50,51] The reaction proceeds by nucleophilic attack of PMe_3 on a π^* orbital of Mo═O. The transition state features a weakened Mo−O bond and a significant O−P interaction, as the spectator Mo═O bond is strengthened. Finally, the rotation of $OPMe_3$ about the Mo−O bond breaks the Mo−O π interaction, resulting in the formation of O═PMe_3 as a ligand on Mo^{IV}.

The similarities between the OAT mechanisms of rhenium and molybdenum cannot be missed (see Schemes 1 and 2). We shall now relate our rhenium system to a representative group of molybdenum model complexes. One drawback in obtaining functional models of molybdenum enzymes has been the facile coproportion of $Mo^{IV}(O)$ and $Mo^{VI}(O)_2$ complexes to give μ-oxo Mo^{V} dimers. Holm and co-workers employed sterically demanding ligands and described the first catalytic model system involving dioxo Mo^{VI} and monooxo Mo^{IV}.[52,53] The rate constants for a few OAT reactions with these Mo complexes are presented in Table 5.[14,15] Young studied the kinetics of another system based on complexes of the type $(HBpz_3)Mo^{IV}(O)(S_2PR_2)$.[16,17,54] Among the highest rate constants recorded for Young's complexes are those included in Table 5.[16] Albeit that the ligand systems are different, the rates of OAT with rhenium are several orders of magnitude higher than those reported for molybdenum (Table 5). For example, the rate of OAT from Ph_2SO to $[(hoz)_2Re(O)(H_2O)][OTf]$, **2**, is ∼60000× that to $(^tBuL\text{-}NS)_2Mo(O)$ (entries 1 and 5 in Table 5). Similarly, the second-order

(44) Seymore, S. B.; Brown, S. N. *Inorg. Chem.* **2000**, *39*, 325−332.
(45) Pomp, C.; Wieghardt, K. *Polyhedron* **1988**, *7*, 2537−2542.
(46) Brown, S. N.; Mayer, J. M. *Inorg. Chem.* **1992**, *31*, 4091−4100.
(47) Hammett, L. P. *Physical Organic Chemistry*; McGraw-Hill Book Co.: New York, 1940; pp 184−228.
(48) Hansch, A.; Leo, T. R. *Chem. Rev.* **1991**, *91*, 165−195.
(49) Xu, L.; Setyawati, I. A.; Pierreroy, J.; Pink, M.; Young, V. G.; Patrick, B. O.; Rettig, S. J.; Orvig, C. *Inorg. Chem.* **2000**, *39*, 5958−5963.
(50) Pietsch, M. A.; Hall, M. B. *Inorg. Chem.* **1996**, *35*, 1273−1278.
(51) Pietsch, M. A.; Couty, M.; Hall, M. B. *J. Phys. Chem.* **1995**, *99*, 16315−16319.
(52) Berg, J. M.; Holm, R. H. *J. Am. Chem. Soc.* **1985**, *107*, 917−925.
(53) Harlan, E. W.; Berg, J. M.; Holm, R. H. *J. Am. Chem. Soc.* **1986**, *108*, 6992−7000.
(54) Roberts, S. A.; Young, C. G.; Cleland, W. E.; Ortega, R. B.; Enemark, J. H. *Inorg. Chem.* **1988**, *27*, 3044−3051.

Table 5. Rates of Oxygen Atom Transfer Reactions with Molybdenum and Rhenium[a]

entry	reaction[b]	k/L mol^{-1} s^{-1}	ref
1	(^{t}BuL-NS)$_2$Mo^{IV}(O) + Ph_2SO → (^{t}BuL-NS)$_2$Mo^{VI}(O)$_2$ + Ph_2S	3.14×10^{-4}	15
2	(^{t}BuL-NS)$_2$Mo^{IV}(O) + Ph_3AsO → (^{t}BuL-NS)$_2$Mo^{VI}(O)$_2$ + Ph_3As	5.6×10^{-2}	15
3	(L-pz$_3$)Mo^{IV}(O)(S_2PPr_2) + Me_2SO → (L-pz$_3$)Mo^{VI}(O)$_2$(S_2PPr_2) + Me_2S	5.5×10^{-5}	16
4	(L-pz$_3$)Mo^{IV}(O)(S_2PPr_2) + Py*N*O → (L-pz$_3$)Mo^{VI}(O)$_2$(S_2PPr_2) + Py	4.8×10^{-4}	16
5	[(hoz)$_2$Re^{V}(O)]$^+$ + Ph_2SO → [(hoz)$_2$Re^{VII}(O)$_2$]$^+$ + Ph_2S	20 (T = 23 °C)	this work
6	(^{t}BuL-NS)$_2$Mo^{IV}(O)$_2$ + Et_3P → (^{t}BuL-NS)$_2$Mo^{VI}(O) + Et_3PO	5.6×10^{-3}	15
7	(L-NS$_2$)Mo^{VI}(O)$_2$ + (p-$C_6H_4F)_3P$ → (L-NS$_2$)Mo^{IV}(O) + (p-$C_6H_4F)_3PO$	9.7×10^{-3}	14
8	(L-pz$_3$)Mo^{VI}(O)$_2$(S_2PPr_2) + Ph_3P → (L-pz$_3$)Mo^{IV}(O)(S_2PPr_2) + Ph_3PO	2.5×10^{-4} (T = 30 °C)	16
9	[(hoz)$_2$Re^{VII}(O)$_2$]$^+$ + Et_2S → [(hoz)$_2$Re^{V}(O)]$^+$ + Et_2SO	2.5 (T = 23 °C)	this work

[a] Rate constants were measured at 25 °C unless specified otherwise. [b] Key to ligand abbreviations: (^{t}BuL-NS) = bis-(4-*tert*-butylphenyl)-2-pyridylmethanethiolate; L-pz$_3$ = hydrotris(3,5-dimethylpyrazol-1-yl)borate; hoz = 2-(2′-hydroxyphenyl)-2-oxazoline; L-NS$_2$ = dianion of 2,6-bis(2,2-diphenyl-2-mercaptoethyl)pyridine.

rate constant for oxidation of Et_2S with [(hoz)$_2$Re(O)$_2$][OTf], **3**, is ∼260× that for the oxidation of (p-$C_6H_4F)_3P$ with (L-NS$_2$)Mo(O)$_2$, despite the larger bond energy of R_3P═O (entries 7 and 9 in Table 5).

If in the transition state there is substantial Re^{VII}═O bond stretching (vide supra), the metal oxo bond strength should contribute to the activation enthalpy. The Re^{VII}═O bond strength in [Re(O)$_2$(hoz)$_2$]$^+$, **3**, (∼20 kcal/mol) is smaller than the identified range for Mo^{VI}═O (32−42 kcal/mol) in enzymes and model complexes.[55] Thus, the higher oxidizing ability of rhenium from a thermodynamic standpoint might be in part responsible for its kinetic superiority over molybdenum in OAT reactions. However, such arguments would predict reversal in the trend ($k_{Mo} > k_{Re}$) for reactions of XO with Mo^{IV}(O) and Re^{V}(O), since the formation of Mo^{VI}(O)$_2$ is more favorable thermodynamically. Entries 1 and 5 in Table 5 (k_{Re}/k_{Mo} = 64000) demonstrate clearly that factors other than thermodynamics are responsible for the observed kinetics. (^{t}BuL-NS)$_2$Mo(O) reacts with Ph_3AsO, Table 5 ($Ph_3AsO \rightarrow Ph_3As + {}^1/_2O_2$, $\Delta G° = 48$ kcal mol^{-1}), a fact that places a lower limit on the dissociation energy of (^{t}BuL-NS)$_2$Mo(O)$_2$ (>48 kcal mol^{-1}). Structural differences between [(hoz)$_2$Re(O)(OH$_2$)]$^+$ (**2**) and [(hoz)$_2$Re(O)$_2$]$^+$ (**3**) as well as reorganizational changes associated with substrate binding possibly define the kinetics of this system.

In closing, the compelling similarities in OAT mechanisms of Re^{V}(O)/Re^{VII}(O)$_2$ and Mo^{IV}(O)/Mo^{VI}(O)$_2$ combined with the higher kinetic competency of rhenium raise the question of why did nature select Mo in oxotransferase proteins? Was the choice dictated by the relative abundance of these metals in nature? In molybdenum-deficient environments, tungsten enzymes have been realized in thermophilic bacteria.[56,57] Could rhenium-dependent enzymes (oxotransferases) exist in biology, or could they be manufactured under artificial conditions in which the organism's growth medium contains rhenium instead of molybdenum?

(55) Lippard, S. J.; Berg, J. M. *Principles of Bioinorganic Chemistry*; University Science Books: Mill Valley, CA, 1994; p 324.
(56) Chan, M. K.; Mukund, S.; Kletzin, A.; Adams, M. W. W.; Rees, D. C. *Science* **1995**, *267*, 1463−1469.
(57) Johnson, M. K.; Rees, D. C.; Adams, M. W. W. *Chem. Rev.* **1996**, *96*, 2817−2840.

Summary

Oxygen atom transfer reactions with sulfoxides are catalyzed efficiently by oxorhenium(V) oxazoline complexes, [(hoz)$_2$Re(O)Cl] (**1**) and [(hoz)$_2$Re(O)(OH$_2$)][OTf] (**2**). The mechanism involves the formation of a cationic dioxorhenium(VII) complex, [(hoz)$_2$Re(O)$_2$][OTf] (**3**), that possesses highly electrophilic oxo ligands. The formation of the dioxo intermediate is facilitated by the availability of an open-coordination site on rhenium(V). The donation of an oxygen atom from **3** to sulfides proceeds via a transition state which features positive charge buildup on sulfur and displays a pronounced sensitivity to electronic effects. Surprisingly, the rate of reactions of **3** with sulfides is not influenced by sterics; the bulky $^tBu_2S$ is slightly less reactive than Me_2S. The oxotransferase mechanism(s) described here for rhenium parallel those characterized for Mo^{IV}(O)/Mo^{VI}(O)$_2$ complexes that model molybdenum enzymes. A comparison of the kinetics studied here for rhenium with analogous molybdenum systems does not produce any correlation that could be rationalized based on known thermodynamic parameters. Thus, it was concluded that the kinetics of OAT must be governed by structural changes and substrate binding. In the presence of water, the cationic dioxorhenium(VII) hydrolyzes to give the neutral trioxorhenium(VII), which exhibits no catalytic activity toward OAT reactions.

Acknowledgment. Financial support from the National Science Foundation (CHE-9874857-CAREER), the Arnold and Mabel Beckman Foundation (Young Investigator Award to M.M.A.-O.), and the University of California is gratefully acknowledged. We thank Dr. Saeed Khan for his assistance with the X-ray structural analysis and Mr. Gregory Owens for preparing complex **5**.

Supporting Information Available: Crystallographic tables for complex **2**: atomic coordinates and equivalent isotropic displacement parameters (Table S1), bond lengths and angles (Table S2), anisotropic displacement parameters (Table S3), and hydrogen coordinates and isotropic displacement parameters (Table S4). Kinetic traces for the oxidation of Me_2S with Ph_2SO as catalyzed by complexes **1** and **2** (Figure S1). A plot of k_ψ vs [Re]$_T$ (Figure S2). This material is available free of charge via the Internet at http://pubs.acs.org.

IC000917Z